Hindawi Publishing Corporation
Mathematical Problems in Engineering
Volume 2014, Article ID 719803, 11 pages
http://dx.doi.org/10.1155/2014/719803

Research Article

Wind Turbine Pitch Control and Load Mitigation Using an L_1 Adaptive Approach

Danyong Li,[1] Yongduan Song,[1,2] Wenchuan Cai,[1] Peng Li,[1] and Hamid R. Karimi[3]

[1] *School of Electronic and Information Engineering, Beijing Jiaotong University, Beijing 100044, China*
[2] *School of Automation, Chongqing University, Chongqing 400044, China*
[3] *Department of Engineering, University of Agder, 4898 Grimstad, Norway*

Correspondence should be addressed to Wenchuan Cai; wchcai@bjtu.edu.cn

Received 26 February 2014; Revised 12 March 2014; Accepted 16 March 2014; Published 16 April 2014

Academic Editor: Weichao Sun

We present an application of L_1 adaptive output feedback control design to wind turbine collective pitch control and load mitigation. Our main objective is the design of an L_1 output feedback controller without wind speed estimation, ensuring that the generator speed tracks the reference trajectory with robustness to uncertain parameters and time-varying disturbances (mainly the uniform wind disturbance across the wind turbine rotor). The wind turbine model CART (controls advanced research turbine) developed by the national renewable energy laboratory (NREL) is used to validate the performance of the proposed L_1 adaptive controller using the FAST (fatigue, aerodynamics, structures, and turbulence) code. A comparative study is also conducted between the proposed controller and the most popular methods in practice: gain scheduling PI (GSPI) controls and disturbance accommodating control (DAC) methods. The results show better performance of L_1 output feedback controller over the other two methods. Moreover, based on the FAST software and LQR analysis in the reference model selection of L_1 adaptive controller, tradeoff can be achieved between control performance and loads mitigation.

1. Introduction

Wind turbine power output should be maintained at a rated value when operating in region 3 [1]. For a variable-speed machine, a constant torque is applied to the generator, and the turbine rotational speed is maintained at a desired value through blade pitching. As wind turbines become larger and more flexible, the degree of coupling between flexible modes increases. It is important to look for advanced control strategies to achieve increased performance in pitch control.

One of the most popular pitch control strategies used in large commercial wind turbines is the gain scheduling proportional integral (GSPI) control [2–5]. However, the disadvantage of this classical control method is that multiple control loops must be used to simultaneously stabilize several flexible turbine modes. If these control loops are not designed carefully, they may interfere with or even excite each other, eventually leading to divergence.

Another popular pitch control strategy is the disturbance accommodating control (DAC) method. Based on state-space model, DAC can reject wind disturbance and mitigate loads by increasing the damping of the first front-aft tower vibration mode and the drive chain torsion mode [4, 5]. However, since the operating environments are time varying, control performance will not be guaranteed when the turbine is not working near the selected operating points where the DAC controller is designed.

As opposed to linear control methods, adaptive control allows for performance over a wider uncertain operating environment. The main nonlinearities in a wind turbine model come from the nonlinear aerodynamic loads on the turbine, making it extremely difficult to create an accurate model of its dynamical characteristics. In addition, wind turbines operate in highly turbulent and unpredictable conditions. These complex aspects of wind turbines make them attractive candidates for the application of adaptive control methods [6–8].

There are several applications of adaptive methods to wind turbine pitch control. Nonlinear memory-based pitch controller was presented in [1], which did not require the estimation of wind speed and worked well under modeling uncertainties and external disturbances. However, this method requires knowing several system parameters and it does not consider the effort of system loads. Model predictive control was presented in [9, 10], which estimated states and switched between different MPC controllers. Direct adaptive collective pitch controller was designed in [2, 3, 11], which can adaptively handle uncertain parameters and reject step disturbances. Some advanced controllers such as H_∞ are also used to deal with the load mitigation [12, 13]. However, to the authors' knowledge, L_1 adaptive control has not yet been applied to the wind turbine control problem.

L_1 adaptive control has some key characteristics that make it an appealing control strategy [14–16]. One characteristic is that it has guaranteed robustness in the presence of fast adaptation, which is necessary for accommodating rapid variations in uncertainty and achieving desired performance. This is obtained by formulating the control objective in a manner that takes into consideration that the uncertainties in any real world system can only be compensated for within the available bandwidth of the control channel. Thus, it is possible to decouple the adaptation from the control of the system. In the case of L_1 adaptive control, fast adaptation is beneficial both for robustness and performance. L_1 adaptive control has been successfully used in UAV systems [17–20], drilling systems [21], and other industry systems.

The focus of this paper is on designing a wind turbine pitch control strategy using L_1 adaptive output feedback control, which ensures stable performance in the presence of model uncertainties, achieves desired reference tracking objectives, and is capable of adapting rapidly to variations in system model parameters. By carefully choosing the reference model based on LQR technology, tradeoff between control performance and loads mitigation can be achieved. The adaptive controller was implemented in the FAST simulation of the CART and tested with step wind inflow and turbulent wind inflow. Comparisons of the normalized generator speed errors were then made among the three controllers: L_1 adaptive controller, GSPI, and DAC pitch controllers.

2. Wind Turbine Modeling

Nonlinear dynamic model of a wind turbine is difficult to build. If the model is too simple, important dynamics will be excluded, possibly leading to reduced performance or even unstable closed-loop system. On the other hand, an overly complex model will make it rather complicated and difficult to design, implement, and test the control system in practice. The FAST software provides feasible wind turbine model, assuming that the most important turbine dynamics can be modeled with about 22 degree of freedoms [22]. The beauty of FAST is that different DOFs can be switched on or off. This means that linear models containing a subset of the total DOFs modeled with FAST can be extracted. Based on these models, classical control methods can be easily used to design controllers that render a stable closed-loop system. Furthermore, adaptive controllers can be designed to compensate for time-varying parameters and external disturbances.

The linearization process using FAST code consists of two steps: computing a periodic steady state operating point for the DOFs and numerically linearizing the FAST model at this operating point to obtain periodic state matrices.

2.1. Periodic Steady State Solution. The first step in linearization is to determine an operating point about which FAST calculates linearized state matrices. An operating point is a set of values of displacements, velocities, accelerations, control inputs, and wind inputs that characterize a steady condition of the wind turbine. For a wind turbine operating in steady wind, this operating point is periodic: values of the operating point depend on the rotor azimuth orientation. This periodicity is driven by aerodynamic loads, which depend on the rotor azimuth position in the presence of prescribed shaft tilt, wind shear, yaw error, or tower shadow. Gravitational loads also drive the periodic behavior when there is a prescribed shaft tilt or appreciable deflection of the tower due to thrust loading. For control design, periodic linear models are generated at several points around the rotor disk and averaged with respect to blade azimuth position to obtain a state-space model [22]. The periodic steady state computation diagram is shown in Figure 1.

2.2. Model Linearization. Once a periodic steady-state solution is found, FAST will numerically linearize the complete nonlinear model at this operating point.

The complete nonlinear aeroelastic equations of motion modeled in FAST can be written as

$$M\left(q,u,t\right)\ddot{q} + f\left(q,\dot{q},u,u_d,t\right) = 0, \tag{1}$$

where M is the mass matrix, f is the nonlinear "forcing function" vector, q is the vector of displacements, $\dot{q}$ and $\ddot{q}$ are the velocities and accelerations, u is the vector of control inputs, u_d is the vector of wind input "disturbances," and t is time. Note that in the steady state solution, only the displacement, velocity, and acceleration vectors are periodic with the rotor azimuth position. The vector of control inputs and the vector of wind disturbances are not periodic.

FAST numerically linearizes the aeroelastic equations of motion by perturbing (represented by a Δ) each of the system variables about their respective operating point (op) values:

$$\begin{gathered} q = q_{\text{op}} + \Delta q, \qquad \dot{q} = \dot{q}_{\text{op}} + \Delta\dot{q}, \qquad \ddot{q} = \ddot{q}_{\text{op}} + \Delta\ddot{q}, \\ u = u_{\text{op}} + \Delta u, \qquad u_d = u_{\text{dop}} + \Delta u_d. \end{gathered} \tag{2}$$

Substituting these expressions into equations of motion (1) and performing Taylor expansions, ignoring higher order terms, an approximate second-order linearized equation of motion is obtained as

$$M\Delta\ddot{q} + C\Delta\dot{q} + K\Delta\dot{q} = F\Delta u + F_d\Delta u_d, \tag{3}$$

where $M = M|_{\text{op}}$ is the mass matrix, $C = (\partial f/\partial\dot{q})_{\text{op}}$ is the damping matrix, $K = [(\partial M/\partial q)\ddot{q} + \partial f/\partial q]_{\text{op}}$ is the stiffness

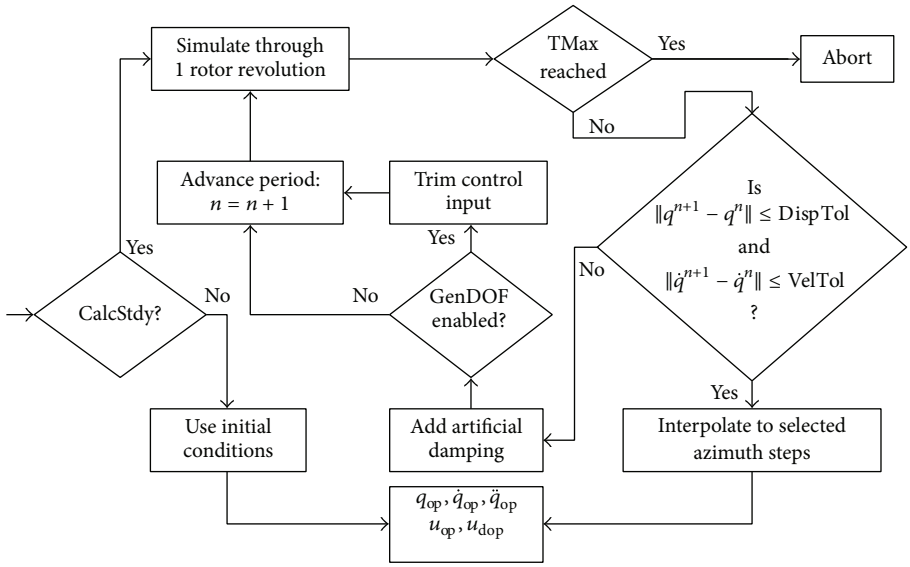

Figure 1: Periodic steady state computation.

matrix, $F = -[(\partial M/\partial u)\ddot{q} + \partial f/\partial u]_{op}$ is the control input matrix, and $F_d = -(\partial f/\partial u_d)_{op}$ is the wind input disturbance matrix.

The subscript "|op" is used to signify that the partial derivatives are taken at the operating point. Along with the linearized equations of motion, FAST also develops a linearized system associated with output measurements Δy. The system output is written as follows:

$$\Delta y = \text{VelC} \cdot \Delta\dot{q} + \text{DspC} \cdot \Delta q + D\Delta u + D_d \Delta u_d, \quad (4)$$

where Vel$C$ is the velocity output matrix, Dsp$C$ is the displacement output matrix, D is the control input transmission matrix, and D_d is the wind input disturbance transmission matrix.

Let $\Delta x = \left[\Delta q \;\; \Delta\dot{q}\right]^T$, which leads to a state-space model:

$$\begin{aligned} \Delta\dot{x} &= A\Delta x + B\Delta u + B_d \Delta u_d, \\ \Delta y &= C\Delta x + D\Delta u + D_d \Delta u_d. \end{aligned} \quad (5)$$

The state matrix A, control input matrix B, wind input disturbance matrix B_d, and output state matrix C are computed as

$$\begin{aligned} A &= \begin{bmatrix} 0 & I \\ -M^{-1}K & -M^{-1}C \end{bmatrix}, \qquad B = \begin{bmatrix} 0 \\ M^{-1}F \end{bmatrix}, \\ B_d &= \begin{bmatrix} 0 \\ M^{-1}F_d \end{bmatrix}, \qquad C = \left[\text{DspC} \;\; \text{VelC}\right], \end{aligned} \quad (6)$$

where I is the identity matrix and 0 is a matrix of zeros.

Since the operating point is periodic with the rotor azimuth position, the linearized representation of the model is also periodic. FAST uses a special averaging tool described in [22] to obtain a more accurate model.

3. L_1 Adaptive Pitch Controller

This section presents an overview of the L_1 adaptive output feedback controller and its application to above generic flexible wind turbine model. The L_1 adaptive control architecture was first presented by Cao and Hovakimyan in [15] for systems with constant unknown parameters using a state feedback approach. An output feedback extension was then presented for a class of uncertain systems allowing for tracking arbitrary reference systems, without imposing an SPR-type requirement on its input-output transfer function. The L_1 adaptive controller ensures uniform transient performance for system's input and output, independent of the unknown nonlinearities and system model. Unlike many other adaptive control strategies, in the L_1 adaptive control, the adaptation rate is decoupled from robustness, leading to easier tradeoff between performance and robustness by choosing appropriate low pass filter on adaptive control signals. It is this particular architecture that is employed in this paper to address the control challenge of the flexible wind turbine model.

Consider the following single-input single-output (SISO) system:

$$y(s) = A(s)\left(u(s) + d(s)\right), \quad (7)$$

where $u(t) \in \mathbb{R}$ is the control input, $y(t) = \mathbb{R}$ is the system output, $A(s)$ is a strictly proper unknown transfer function of unknown relative degree n_r for which only a known lower bound $1 < d_r \le n_r$ is available, and $d(s)$ is the Laplace transform of the time-varying uncertainties and disturbances $d(t) = f(t, y(t))$, where $f(\cdot)$ is an unknown, possibly nonlinear function, representing the deviations of the plant from the model $A(s)$.

Let $r(t)$ be a given bounded continuous reference input signal. The objective is to design an adaptive output feedback

controller $u(t)$ such that the system output $y(t)$ tracks the reference input $r(t)$ following a desired model:

$$y_d(s) = M(s) r(s), \tag{8}$$

where $M(s)$ is a minimum-phase stable transfer function of relative degree $d_r > 1$. The system equations in terms of the desired model can be rewritten as

$$y(s) = M(s)(u(s) + \sigma(s)), \tag{9}$$

where

$$\sigma(s) = \frac{((A(s) - M(s))u(s) + A(s)d(s))}{M(s)}. \tag{10}$$

Next we introduce a closed-loop reference system, defining an achievable control objective for the L_1 adaptive controller.

The closed-loop reference system is given by

$$\begin{aligned} y_{\text{ref}}(s) &= M(s)\left(u_{\text{ref}}(s) + \sigma_{\text{ref}}(s)\right), \\ \sigma_{\text{ref}}(s) &= \frac{\left((A(s) - M(s))u_{\text{ref}}(s) + A(s)d_{\text{ref}}(s)\right)}{M(s)}, \\ u_{\text{ref}}(s) &= C(s)\left(r(s) - \sigma_{\text{ref}}(s)\right), \end{aligned} \tag{11}$$

where $C(s)$ is a low pass filter with DC gain $C(0) = 1$ and $d_{\text{ref}}(t) = f(t, y_{\text{ref}}(t))$.

The selection of $C(s)$ and $M(s)$ must ensure that

$$H(s) = \frac{A(s)M(s)}{(C(s)A(s) + (1 - C(s))M(s))} \tag{12}$$

is stable and the following L_1 norm condition is satisfied:

$$\|H(s)(1 - C(s))\|_{L_1} L < 1. \tag{13}$$

Then, the reference system in (8) is stable.

Elements of the L_1 adaptive controller are introduced next.

State Predictor. Let $(A_m \in \mathbb{R}^{n\times n}, b_m \in \mathbb{R}^n, c_m \in \mathbb{R}^n)$ be the minimal realization of $M(s)$. Hence, (A_m, b_m, c_m) is controllable and observable with A_m being Hurwitz. Then, the system in (7) can be rewritten as

$$\begin{aligned} \dot{x}(t) &= A_m x(t) + b_m(u(t) + \sigma(t)), \\ y(t) &= c_m^T x(t). \end{aligned} \tag{14}$$

The state predictor is given by

$$\begin{aligned} \dot{\widehat{x}}(t) &= A_m \widehat{x}(t) + b_m u(t) + \widehat{\sigma}(t) \\ \widehat{y}(t) &= c_m^T \widehat{x}(t), \end{aligned} \tag{15}$$

where $\widehat{\sigma}(t) \in \mathbb{R}$ is the vector of adaptive parameters. Notice that in the state predictor equations $\widehat{\sigma}(t)$ is not in the span of b_m, while in (14) $\widehat{\sigma}(t)$ is in the span of b_m. Further, let $\widetilde{y}(t) = \widehat{y}(t) - y(t)$.

Adaptation Law. Let P be the solution of the following algebraic Lyapunov equation:

$$A_m^T P + P A_m = -Q, \tag{16}$$

where $Q > 0$. From the properties of P it follows that there always exists a nonsingular $\sqrt{P}$ such that

$$P = \sqrt{P}^T \sqrt{P}. \tag{17}$$

Given the vector $c_m^T(\sqrt{P})^{-1}$, let D be the $(n-1)\times n$ dimensional null space of $c_m^T(\sqrt{P})^{-1}$; that is,

$$D\left(c_m^T\left(\sqrt{P}\right)^{-1}\right)^T = 0, \tag{18}$$

and further let

$$\Lambda = \begin{bmatrix} c_m^T \\ D\sqrt{P} \end{bmatrix} \in \mathbb{R}^{n\times n}. \tag{19}$$

From the definition of the null space, it follows that

$$\Lambda\left(\sqrt{P}\right)^{-1} = \begin{bmatrix} c_m^T(\sqrt{P})^{-1} \\ D \end{bmatrix} \tag{20}$$

is full rank, and hence Λ^{-1} exists.

Let T_s be an arbitrary positive constant, which can be associated with the sampling rate of available CPU, $\mathbf{1}_1 = [1, 0, \ldots, 0]^T \in \mathbb{R}$, and $\widetilde{y}(t) = \widehat{y}(t) - y(t)$. Then, the update law for $\widehat{\sigma}(t)$ is given by

$$\begin{aligned} \widehat{\sigma}(t) &= \widehat{\sigma}(iT_s), \quad t \in [iT_s, (i+1)T_s), \\ \widehat{\sigma}(iT_s) &= -\Phi^{-1}(T_s)\mu(iT_s), \quad i = 1, 2, \ldots, \end{aligned} \tag{21}$$

where

$$\begin{aligned} \Phi(T_s) &= \int_0^{T_s} e^{\Lambda A_m \Lambda^{-1}(T_s - \tau)} \Lambda d\tau, \\ \mu(iT_s) &= e^{\Lambda A_m \Lambda^{-1} T_s} \mathbf{1}_1 \widetilde{y}(iT_s), \quad i = 1, 2, \ldots \end{aligned} \tag{22}$$

Control Law. The control law is defined via the output of the low pass filter:

$$u(s) = C(s) r(s) - \frac{C(s)}{M(s)} c_m^T (sI - A_m)^{-1} \widehat{\sigma}(s). \tag{23}$$

The complete L_1 adaptive controller consists of the state predictor in (15), the adaptation law in (21), and the control law in (23), with the L_1-norm condition in (13). Performance bounds of the L_1 adaptive controller are given by [15]

$$\begin{aligned} \lim_{T\to 0} \|\widetilde{y}\|_{L_\infty} &= 0, \\ \lim_{T\to 0} \|y - y_{\text{ref}}\|_{L_\infty} &= 0, \\ \lim_{T\to 0} \|u - u_{\text{ref}}\|_{L_\infty} &= 0, \end{aligned} \tag{24}$$

where T is the sampling time.

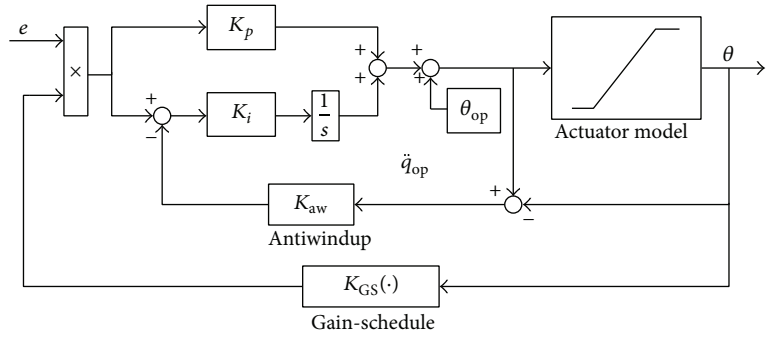

Figure 2: Closed-loop system with the GSPI controller.

Note that the L_1 reference system depends on the uncertainties, which implies that this reference system cannot be used in implementation. It is only used for analysis purposes. We see that L_1 reference system compensates for the uncertainties and the difference between $A(s)$ and $M(s)$ within the bandwidth of the low pass filter $C(s)$. If $C(s) = 1$, then the reference system becomes identical to the desired system. The tracking error is uniformly bounded by a decreasing function of T, implying that during the transient phase, one can achieve arbitrary improvement of tracking performance by uniformly reducing T. Reducing T imposes hardware (CPU) requirements, indicating that the performance limitations are consistent with the hardware limitations.

4. Simulation

To validate the performance of the proposed method, we conducted numerical simulations on CART based on FAST. Comparisons were then made among the GSPI control, DAC control, and L_1 adaptive control.

The FAST simulations of the CART were run from time 0 to 250 s with an integration step size of 5 ms. The first flapwise blade mode DOF, the drive chain rotational-flexibility DOF, and the generator DOF switches were turned on. The rest DOF switches were turned off. The wind turbine had fixed-yaw with no yaw control. Aerodynamic forces were calculated during the runs. The parametric information for the FAST simulator is available in [5].

4.1. Torque Control. The demanded generator torque τ is given by [5]

$$\tau = \begin{cases} 0 & \text{region 1} \\ k_{\text{opt}}\omega^2 & \text{region 2} \\ \tau_1 + \dfrac{\tau_{\text{rated}} - \tau_1}{\omega_{\text{rated}} - \omega_1}\left(\omega - \omega_1\right) & \text{region 2} - \dfrac{1}{2} \\ \tau_{\text{rated}} & \text{region 3,} \end{cases} \tag{25}$$

where ω is the generator speed, $k_{\text{opt}} = 0.0008992$ is the torque constant, $\tau_{\text{rated}} = 3524.36$ Nm is the rated torque, $\omega_{\text{rated}} = 1781.98$ rpm is the rated speed, $\omega_1 = 1691.98$ rpm, and $\tau_1 = 2574.23$ Nm is the region 2 torque corresponding to ω_1.

4.2. Model Linearization for Pitch Control. Here, FAST linearization was done at the operating point, where wind speed $v_0 = 18$ m/s, rotor speed $\omega_0 = 41.7$ m/s, and pitch angle $\theta_0 = 11$ deg with the first flapwise blade mode DOF, the drive train rotational flexibility DOF, and the generator DOF switched on. The system model is obtained as follows:

$$\begin{aligned} \Delta\dot{x} &= \begin{bmatrix} 0 & 0 & 0 & 1 & 0 \\ 0 & 0 & 0 & 0 & 1 \\ 419.8 & 0 & -0.55026 & 0 & 0 \\ -507.1 & 0.97075 & 0.48494 & -0.06538 & 0.00479 \\ 730.26 & -197.76 & -11.681 & -11.681 & -7.3153 \end{bmatrix} \Delta x \\ &\quad + \begin{bmatrix} 0 \\ 0 \\ 1.4741e-07 \\ 1.3971 \\ -932.5646 \end{bmatrix} \Delta u + \begin{bmatrix} 0 \\ 0 \\ 3.7591e-09 \\ 0.0184 \\ 13.025 \end{bmatrix} \Delta u_d, \\ \Delta y &= \begin{bmatrix} 0 & 0 & 412.2 & 0 & 0 \end{bmatrix}^T \Delta x. \end{aligned} \tag{26}$$

It is worth mentioning that this is a time-invariant model, and we use it for DAC design. However, in the design of L_1 adaptive controller, it is only used for theoretical analysis and selection of a reasonable reference model and low pass filter to tradeoff control performance and load mitigation.

4.3. GSPI Control. At the operating point $v_0 = 18$ m/s, $\omega_0 = 41.7$ m/s, $\theta_0 = 2.62$ deg; the PI controller gains were chosen as $K_p = 0.2438$, $K_i = 0.1358$. The pitch angle was limited within $[-1, 90]$ deg ($[-0.0175, 1.5708]$ rad) and pitch rate within $[-10, 10]$ deg/s. The scheduling gain was defined as $K_{\text{GS}} = 1/(1 + \theta/2.62)$ and the antiwindup gain K_{aw} was set to 6. Readers can refer to [4] for details. The block diagram is shown in Figure 2.

4.4. Disturbance Accommodating Control. Based on the linearized model in Section 4.2, a disturbance accommodating controller was designed based on LQR and linear control technologies which moved the poles further to the left in the complex plane to improve damping and transient response.

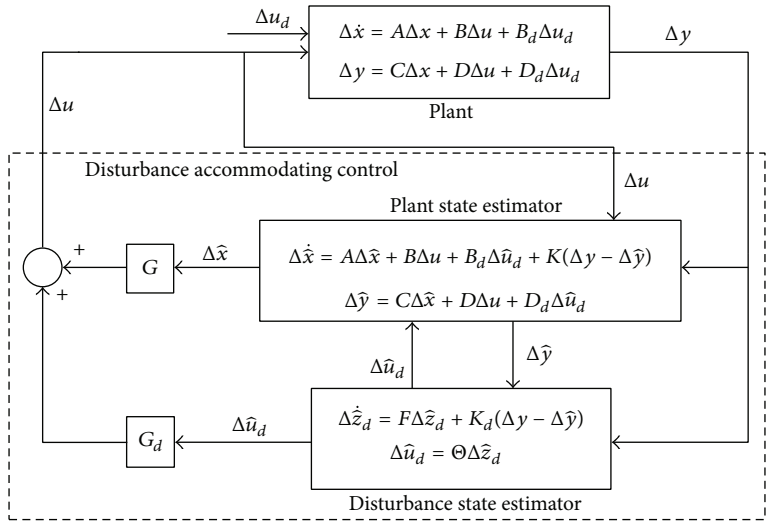

Figure 3: Closed-loop system with the DAC controller.

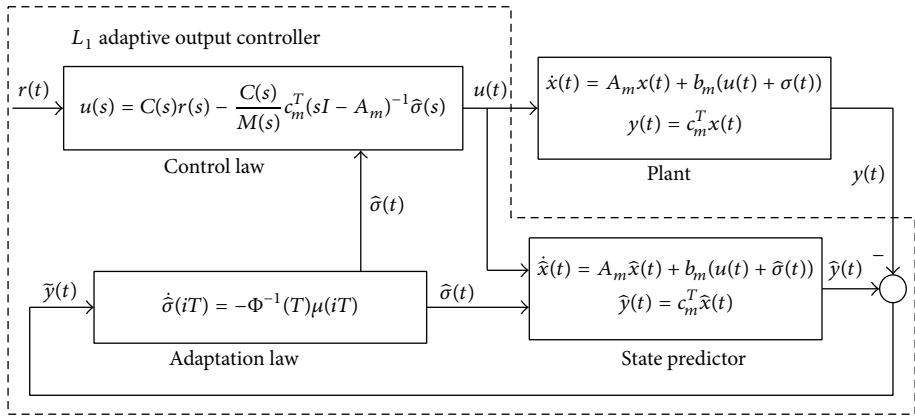

Figure 4: Closed-loop system with the L_1 adaptive output feedback controller.

The resulting gain matrix G was [−14.25 0.04922 0.70936 −0.12904 0.00668] and G_d 0.01397. Details can be found in [4]. The control diagram is shown in Figure 3.

4.5. L_1 Adaptive Output Feedback Control. Following the outline in Section 3, the L_1 adaptive output feedback control architecture is presented in Figure 4.

Selections of the reference model $M(s)$ and low pass filter $C(s)$ have significant impacts on stability and performance of the closed-loop system. This can be seen from the stability criterion of the L_1 adaptive output feedback control formulation, specifically (12) and (13). For wind turbine pitch control problem, $M(s)$ should be selected considering trade-off between tracking errors and loads. Since DAC controller design is based on LQR technology, we can use the model of its closed-loop control system as the desired model $M(s)$ for the L_1 adaptive control design ignoring the disturbance item. Once $M(s)$ was determined, $C(s)$ was then selected to minimize control chatter by filtering out high frequency components of the control signal.

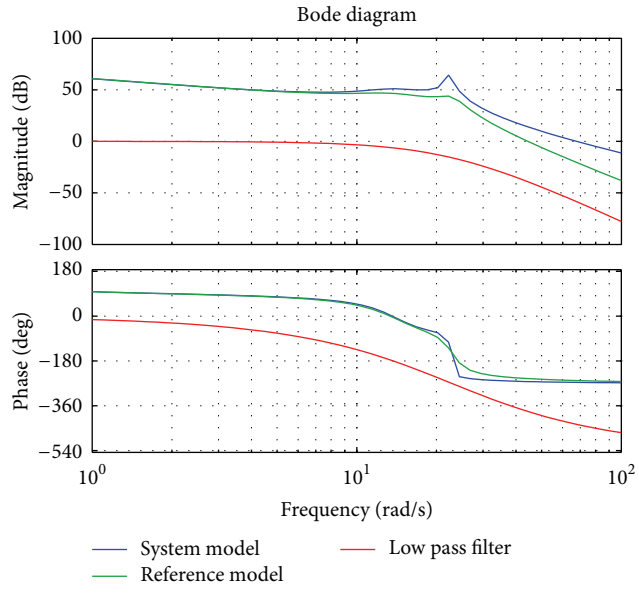

Figure 5: Frequency response of $A(s)$, $M(s)$, and $C(s)$.

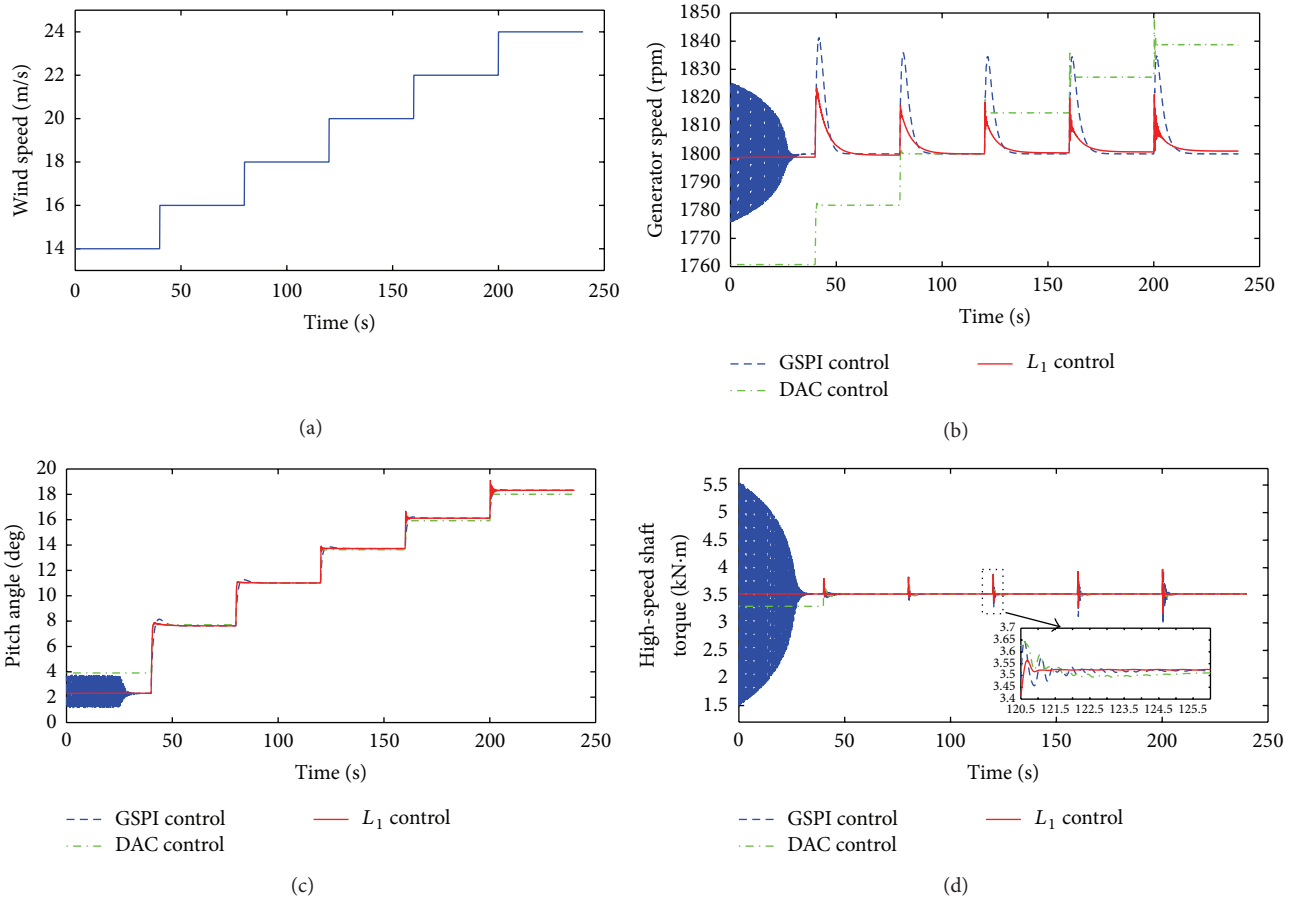

FIGURE 6: Wind speed, generator speed, pitch angle, and high speed shaft torque under the step wind.

Final tuning of $M(s)$ and $C(s)$ was then performed manually until satisfactory performance was achieved. $M(s)$ has the following form:

$$M(s) = K_m \cdot \frac{\omega_{m1}}{s+\omega_{m1}} \cdot \frac{\omega_{m2}^2}{s^2+2\zeta_{m2}\omega_{m2}s+\omega_{m2}^2} \cdot \frac{\omega_{m3}^2}{s^2+2\zeta_{m3}\omega_{m3}s+\omega_{m3}^2}, \quad (27)$$

where $K_m = -5641.6$, $\omega_{m1} = 0.2$ rad/sec, $\omega_{m2} = 22.7$ rad/sec, $\zeta_{m2} = 0.1$, $\omega_{m3} = 13.95$ rad/sec, $\zeta_{m3} = 0.3$. ω_{m1} corresponds to the generator speed mode, ω_{m2} and ζ_{m2} correspond to the first drive chain torsion mode, and ω_{m3} and ζ_{m3} correspond to the first rotor symmetric flapping mode.

The filter $C(s)$ was selected to be of the form

$$C(s) = \left(\frac{\omega_{c1}^2}{s^2+2\zeta_{c1}\omega_{c1}s+\omega_{c1}^2}\right)^2 \cdot \frac{\omega_{c2}^2}{s^2+2\zeta_{c2}\omega_{c2}s+\omega_{c2}^2}, \quad (28)$$

with selected values of $\omega_{c1} = 18$ rad/sec, $\omega_{c2} = 22.5$ rad/sec, and $\zeta_{c1} = \zeta_{c2} = 0.95$.

Figure 5 shows frequency responses of $A(s)$, $M(s)$, and $C(s)$.

Simulations were run with two types of wind inflow to the FAST simulator: step wind and turbulent wind. Generator speed error of each controller was evaluated. The generator speed error is the difference between the generator speed and the rated generator speed, which is 1800 rpm for the CART operating in region 3. A normalized generator speed error for each simulation was then the root mean square (RMS) of speed error from the rated speed [3]. The normalized errors from simulations under different wind speeds are listed in Table 1.

TABLE 1: Normalized generator speed error of the three control methods.

Wind speed	GSPI	DAC	L_1
Step wind	0.0483 rpm	0.1224 rpm	0.0183 rpm
14.5 m/s turbulence wind	0.1042 rpm	0.1576 rpm	0.0908 rpm
19 m/s turbulence wind	0.0924 rpm	0.0885 rpm	0.0413 rpm

4.6. Step Wind. All figures related to the simulations started at time 20 s, after the transients due to system startup are attenuated. The first simulations described in this part had the step wind inflow, which is shown in Figure 6. All of the step wind inflow resulted in region 3 turbine operation. For the step wind, the GSPI, DAC, and L_1 adaptive controller had normalized generator speed errors of 0.0483 rpm,

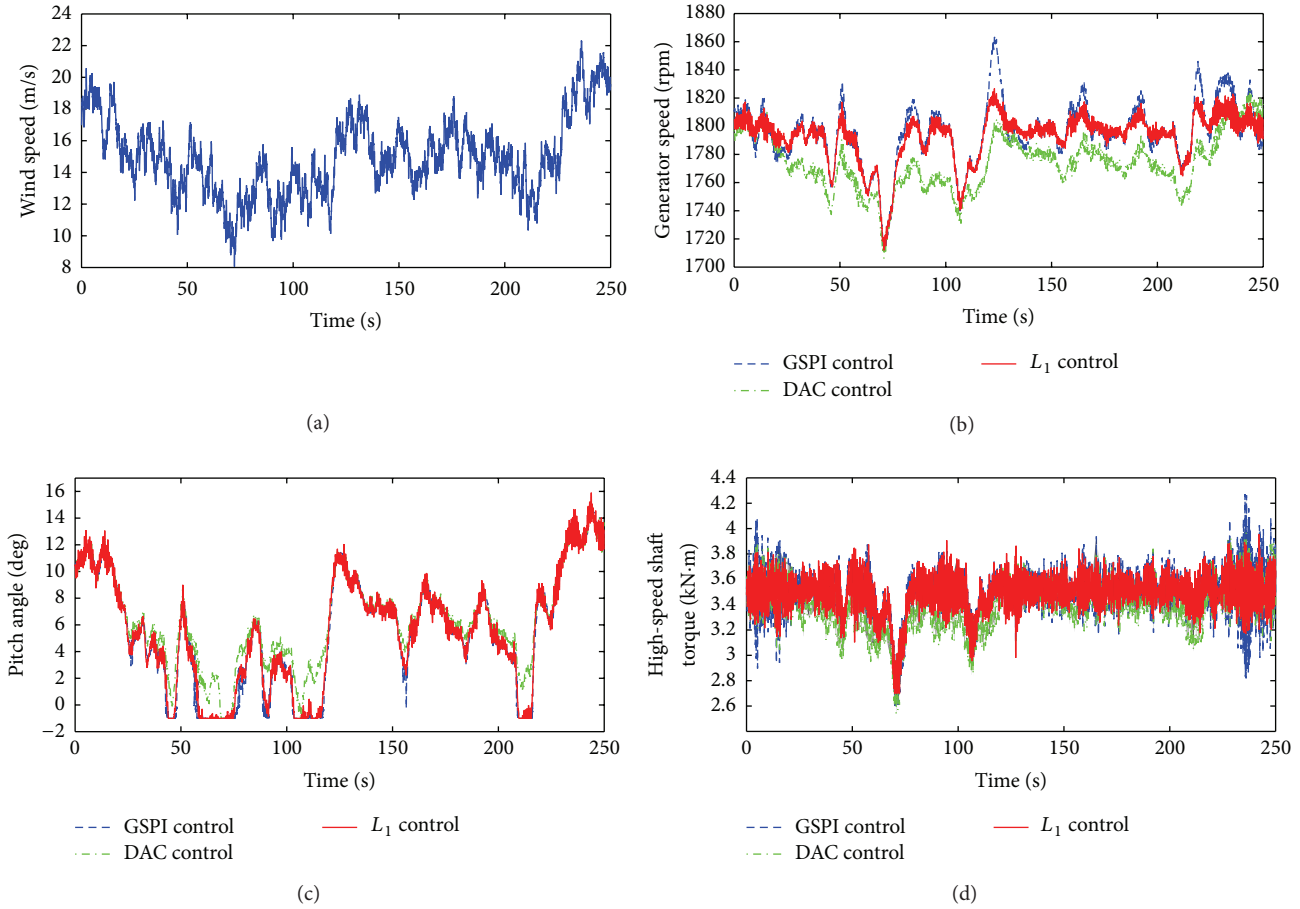

FIGURE 7: Wind speed, generator speed, pitch angle, and high speed shaft torque under the 14.5 m/s turbulence wind.

0.1224 rpm, and 0.0183 rpm, respectively. Since the GSPI and DAC controllers are based on linear control methods, from Figures 6(c) and 6(d), we can find that based on GSPI controller, the generator speed and the high speed shaft torque oscillate heavily with large overshoot, twice the L_1 controller. Under the DAC controller, due to variation of the operational points and external disturbances, the generator speed is not kept about 1800 rpm and even not bounded technically. However, under the L_1 controller, the system is stable and the generator speed is bounded with good transitions.

4.7. Turbulence Wind: 14.5 m/s. A 14.5 m/s turbulent wind inflow to the FAST simulator was used in the second set of simulations; see Figure 7. The turbulent wind inflow speed was below that of the linearization point (18 m/s) in region 3. In this simulation, the GSPI, DAC, and L_1 adaptive controllers had normalized generator speed errors of 0.1042 rpm, 0.1576 rpm, and 0.0908 rpm, respectively. Figure 7(c) shows that when the wind speed is in region 2, under the GSPI control, pitch angle is maintained at −1 deg, so the control performance is good but the drive chain load is adverse; under the DAC controller, the pitch angle is not at −1 deg, so the control performance is not as good but the load is improved; under the L_1 adaptive controller, the pitch angle is almost maintained at −1 deg, with some necessary tuning at certain points to compensate for the disturbance, which is a good example of tradeoff between control performance and loads mitigation.

4.8. Turbulence Wind: 19 m/s. When the turbulent wind inflow was above that of the operating point, simulation results are shown in Figure 8. The GSPI, DAC, and L_1 adaptive controllers had normalized generator speed errors of 0.0924 rpm, 0.0885 rpm, and 0.0413 rpm, respectively. Compared with GSPI and DAC controllers, under the L_1 adaptive controller, the pitch angle changes a little more frequently and its magnitude is a little larger, but still comparable. But the magnitude of the pitch rate is below the limit of $\pm 10^{\circ}$/s prescribed in the CART. Hence, it can compensate for wind turbine uncertainties. In addition, Figure 8(d) indicates that the high speed shaft torque under the L_1 adaptive controller has less chattering than the other two methods.

Figure 9 shows the RMS of generator speed error of the three controllers under turbulence winds with different mean speed. With the mean wind speed increasing, the relative

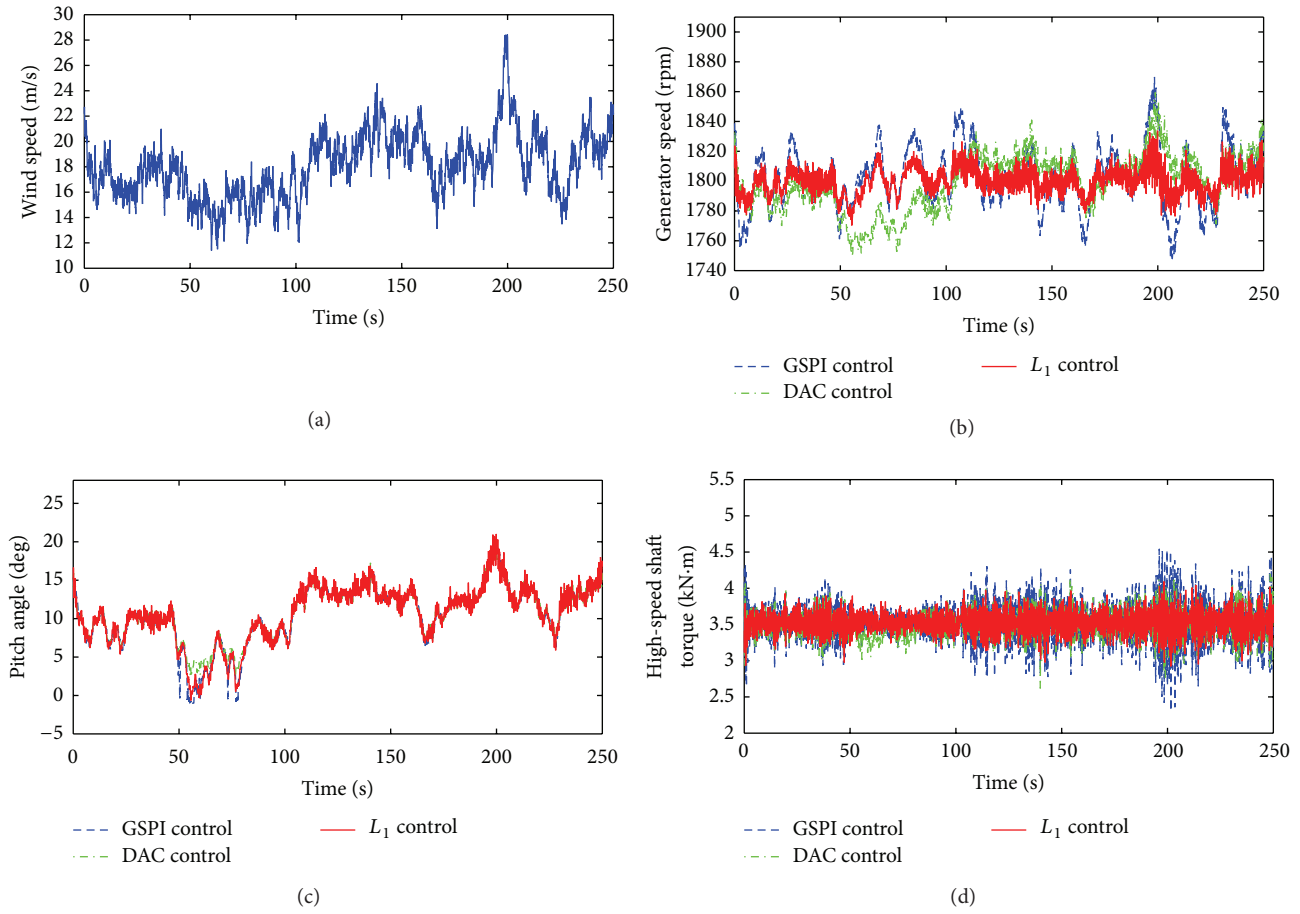

FIGURE 8: Wind speed, generator speed, pitch angle, and high speed shaft torque under the 19 m/s turbulence wind.

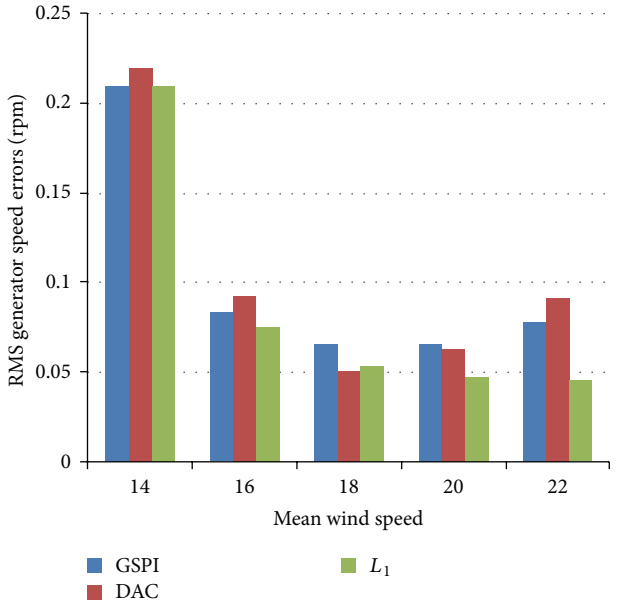

FIGURE 9: RMS of generator speed errors under turbulence winds with different mean speed.

speed control performance of the L_1 adaptive controller to the GSPI controller improves continuously. Eventually it has a significant performance improvements of up to 56% relative to the GSPI controller at 22 m/s. Moreover, it indicates that near the linearization point (18 m/s) the speed regulation performance of the DAC controller is better than the L_1 adaptive controller. The reason is that even though the reference model of the L_1 adaptive controller is the closed-loop system model of the DAC controller, L_1 controller uses the adaptive laws to deal with uncertainties and disturbances to ensure uniform control performance and the low pass filter trades off control performance against robustness. In addition, when the mean wind speed (14 m/s) is in the transition region from region 2 to region 3, the speed regulation performance of the L_1 controller is almost identical to the GSPI controller. Near the transition region, the wind turbine model is quite different from in region 3. In order to achieve a better tradeoff between control performance and robustness in the entire operation region, we choose a reasonable bandwidth for the low pass filter, which might sacrifice some control performance in low wind speed region.

The normalized results of the three controllers under turbulence wind with mean speed of 18 m/s are shown

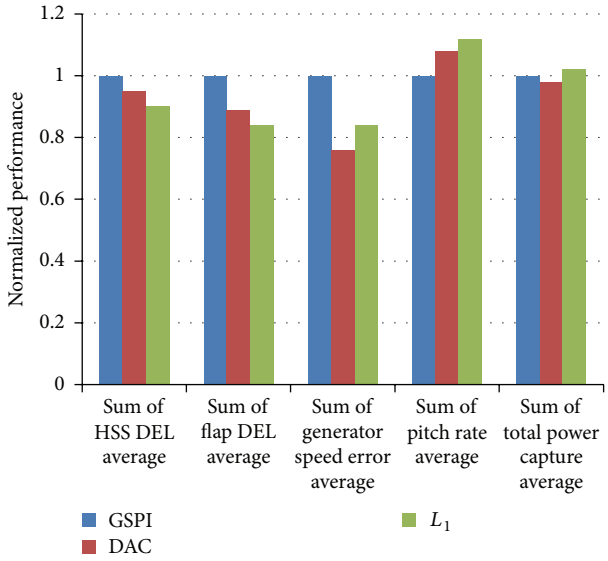

FIGURE 10: Normalized results in turbulence wind with mean speed of 18 m/s.

in Figure 10. Compared with the GSPI controller, the L_1 adaptive controller has almost identical power capture ability and a 16% generator speed error reduction. Meanwhile, the L_1 adaptive controller also shows ability to reduce the HSS DELs (10%) and blade flap DELs (16%). However, there is a 12% increase in pitch rate, mainly due to using the pitch angle adjustment to compensate for the efforts of wind turbine time-varying parameters and disturbances.

5. Conclusion

The proposed L_1 adaptive output feedback controller uses the generator speed only (no need for wind speed estimation) and is robust to wind turbine parameter varying and external wind disturbances. Compared with most existing methods, the proposed one is more user-friendly in control design and easier for real-time implementation. Simulation results on CART model showed promise for improved generator speed regulation. The adaptive pitch controller reduced the generator speed errors compared with the GSPI and DAC controllers in simulations with both step wind and turbulent wind inflow. In further work, an L_1 network voltage control system for large wind farm will be designed.

Conflict of Interests

The authors declare that there is no conflict of interests regarding the publication of this paper.

Acknowledgments

This work was supported in part by the CSC (China Scholarship Council), the Major State Basic Research Development Program 973 (no. 2012CB215202), the National Natural Science Foundation of China (nos. 61134001, 61203124, and 51207007), and State Key Laboratory of Traffic Control and Safety Research Program (no. RCS2011ZT013). The authors appreciate Naira Hovakimyan for her advice about the L_1 adaptive control theory in our paper.

References

[1] Y. D. Song, M. Bikdash, and M. J. Schulz, "Control and health monitoring of variable-speed wind power generation systems," NREL/SR-500-29708, National Renewable Energy Lab., Golden, Colo, USA, 2001.

[2] S. A. Frost, M. J. Balas, and A. D. Wright, "Direct adaptive control of a utility-scale wind turbine for speed regulation," *International Journal of Robust and Nonlinear Control*, vol. 19, no. 1, pp. 59–71, 2009.

[3] S. A. Frost, M. J. Balas, and A. D. Wright, "Modified adaptive control for region 3 operation in the presence of wind turbine structural modes," in *Proceedings of the 48th AIAA Aerospace Sciences Meeting Including the New Horizons Forum and Aerospace Exposition*, pp. 1–12, January 2010.

[4] A. Wright and L. J. Fingersh, "Advanced control design for wind turbines part 1: control design, implementation, and initial tests," NREL/SR-500-46442, National Renewable Energy Lab., Golden, Colo, USA, 2009.

[5] J. Darrow, K. Johnson, and A. Wright, "Design of a tower and drive train damping controller for the three-bladed controls advanced research turbine operating in design-driving load cases," *Wind Energy*, vol. 14, no. 4, pp. 571–601, 2011.

[6] B. Boukhezzar and H. Siguerdidjane, "Nonlinear control of a variable-speed wind turbine using a two-mass model," *IEEE Transactions on Energy Conversion*, vol. 26, no. 1, pp. 149–162, 2011.

[7] B. Beltran, M. E. H. Benbouzid, and T. Ahmed-Ali, "Second-order sliding mode control of a doubly fed induction generator driven wind turbine," *IEEE Transactions on Energy Conversion*, vol. 27, no. 2, pp. 261–269, 2012.

[8] T. Senjyu, R. Sakamoto, N. Urasaki, T. Funabashi, H. Fujita, and H. Sekine, "Output power leveling of wind turbine generator for all operating regions by pitch angle control," *IEEE Transactions on Energy Conversion*, vol. 21, no. 2, pp. 467–475, 2006.

[9] M. Soliman, O. P. Malik, and D. T. Westwick, "Multiple model MIMO predictive control for variable speed variable pitch wind turbines," in *Proceedings of the American Control Conference (ACC '10)*, pp. 2778–2784, July 2010.

[10] D. Q. Dang, Y. Wang, and W. Cai, "Offset-free predictive control for variable speed wind turbines," *IEEE Transactions on Sustainable Energy*, vol. 4, no. 1, pp. 2–10, 2013.

[11] K. E. Johnson and L. J. Fingersh, "Adaptive pitch control of variable-speed wind turbines," *Journal of Solar Energy Engineering*, vol. 130, no. 3, Article ID 031012, 7 pages, 2008.

[12] W. Sun, H. Gao Sr., and O. Kaynak, "Finite frequency $\mathscr{H}_\infty$ control for vehicle active suspension systems," *IEEE Transactions on Control Systems Technology*, vol. 19, no. 2, pp. 416–422, 2011.

[13] W. Sun, Y. Zhao, J. Li, L. Zhang, and H. Gao, "Active suspension control with frequency band constraints and actuator input delay," *IEEE Transactions on Industrial Electronics*, vol. 59, no. 1, pp. 530–537, 2012.

[14] N. Hovakimyan and C. Cao, L_1 *Adaptive Control Theory: Guaranteed Robustness with Fast Adaptation*, vol. 21 of *Advances in Design and Control*, SIAM, Philadelphia, Pa, USA, 2010.

[15] C. Cao and N. Hovakimyan, "Design and analysis of a novel L_1 adaptive control architecture with guaranteed transient performance," *IEEE Transactions on Automatic Control*, vol. 53, no. 2, pp. 586–591, 2008.

[16] C. Cao and N. Hovakimyan, "L_1 adaptive output feedback controller for systems of unknown dimension," *IEEE Transactions on Automatic Control*, vol. 53, no. 3, pp. 815–821, 2008.

[17] N. Hovakimyan, C. Cao, E. Kharisov, E. Xargay, and I. M. Gregory, "L_1 adaptive control for safety-critical systems," *IEEE Control Systems Magazine*, vol. 31, no. 5, pp. 54–104, 2011.

[18] E. Xargay, V. Dobrokhodov, I. Kaminer, A. Pascoal, N. Hovakimyan, and C. Cao, "Time-coordinated path following of multiple heterogeneous vehicles over time-varying networks," *IEEE Control Systems Magazine*, vol. 32, no. 5, pp. 49–73, 2012.

[19] D. Erdos, T. Shima, E. Kharisov, and N. Hovakimyan, "L_1 adaptive control integrated missile autopilot and guidance," in *Proceedings of the AIAA Guidance, Navigation and Control Conference*, pp. 1–16, 2012.

[20] K. K. K. Kim, E. Kharisov, and N. Hovakimyan, "Filter design for L_1 adaptive output-feedback controller," in *Proceedings of IEEE Conference on Decision and Control*, pp. 5653–5658, 2011.

[21] Z. Li, N. Hovakimyan, and G. O. Kaasa, "Bottomhole pressure estimation and adaptive control in managed pressure drilling system," in *Proceedings of the 1st IFAC Workshop on Automatic Control of Offshore Oil and Gas Production*, pp. 128–133, Trondheim, Norway, 2012.

[22] J. M. Jonkman and M. L. Buhl, "FAST user's guide," NREL/EL-500-29798, National Renewable Energy Lab., Golden, Colo, USA, 2005.